



Novel Toxin-Antitoxin Module SlvT-SlvA Regulates Megaplasmid Stability and Incites Solvent Tolerance in *Pseudomonas putida* S12

 Hadiastri Kusumawardhani,^a  David van Dijk,^a  Rohola Hosseini,^a  Johannes H. de Winde^a

^aInstitute of Biology Leiden, Leiden University, Leiden, The Netherlands

ABSTRACT *Pseudomonas putida* S12 is highly tolerant of organic solvents in saturating concentrations, rendering this microorganism suitable for the industrial production of various aromatic compounds. Previous studies revealed that *P. putida* S12 contains the single-copy 583-kbp megaplasmid pTTS12. pTTS12 carries several important operons and gene clusters facilitating *P. putida* S12 survival and growth in the presence of toxic compounds or other environmental stresses. We wished to revisit and further scrutinize the role of pTTS12 in conferring solvent tolerance. To this end, we cured the megaplasmid from *P. putida* S12 and conclusively confirmed that the SrpABC efflux pump is the major determinant of solvent tolerance on the megaplasmid pTTS12. In addition, we identified a novel toxin-antitoxin module (proposed gene names *slvT* and *slvA*, respectively) encoded on pTTS12 which contributes to the solvent tolerance phenotype and is important for conferring stability to the megaplasmid. Chromosomal introduction of the *srp* operon in combination with the *slvAT* gene pair created a solvent tolerance phenotype in non-solvent-tolerant strains, such as *P. putida* KT2440, *Escherichia coli* TG1, and *E. coli* BL21(DE3).

IMPORTANCE Sustainable alternatives for high-value chemicals can be achieved by using renewable feedstocks in bacterial biocatalysis. However, during the bioproduction of such chemicals and biopolymers, aromatic compounds that function as products, substrates, or intermediates in the production process may exert toxicity to microbial host cells and limit the production yield. Therefore, solvent tolerance is a highly preferable trait for microbial hosts in the biobased production of aromatic chemicals and biopolymers. In this study, we revisit the essential role of megaplasmid pTTS12 from solvent-tolerant *Pseudomonas putida* S12 for molecular adaptation to an organic solvent. In addition to the solvent extrusion pump (SrpABC), we identified a novel toxin-antitoxin module (SlvAT) which contributes to short-term tolerance in moderate solvent concentrations, as well as to the stability of pTTS12. These two gene clusters were successfully expressed in non-solvent-tolerant strains of *P. putida* and *Escherichia coli* strains to confer and enhance solvent tolerance.

KEYWORDS genome engineering, RND efflux pump, toxin-antitoxin, megaplasmid, solvent tolerance, industrial biotechnology

One of the main challenges in the production of aromatic compounds is chemical stress caused by the added substrates, pathway intermediates, or products. These chemicals, often exhibiting characteristics of organic solvents, are toxic to microbial hosts and may negatively impact product yields. They adhere to the cell membranes, alter membrane permeability, and cause membrane damage (1, 2). *Pseudomonas putida* S12 exhibits exceptional solvent tolerance characteristics, enabling this strain to withstand toxic organic solvents in saturating concentrations (3, 4). Consequently, a grow-

Citation Kusumawardhani H, van Dijk D, Hosseini R, de Winde JH. 2020. Novel toxin-antitoxin module SlvT-SlvA regulates megaplasmid stability and incites solvent tolerance in *Pseudomonas putida* S12. *Appl Environ Microbiol* 86:e00686-20. <https://doi.org/10.1128/AEM.00686-20>.

Editor Hideaki Nojiri, University of Tokyo

Copyright © 2020 Kusumawardhani et al. This is an open-access article distributed under the terms of the [Creative Commons Attribution 4.0 International license](https://creativecommons.org/licenses/by/4.0/).

Address correspondence to Johannes H. de Winde, j.h.de.winde@biology.leidenuniv.nl.

Received 23 March 2020

Accepted 27 April 2020

Accepted manuscript posted online 1 May 2020

Published 17 June 2020

ing list of valuable compounds has successfully been produced using *P. putida* S12 as a biocatalyst by exploiting its solvent tolerance (5–9).

Following the completion of its full-genome sequence and subsequent transcriptome and proteome analyses, several genes have been identified that may play important roles in controlling and maintaining solvent tolerance of *P. putida* S12 (10–12). As previously reported, an important solvent tolerance trait of *P. putida* S12 is conferred through the resistance-nodulation-division (RND)-family efflux pump SrpABC, which actively removes organic solvent molecules from the cells (13, 14). Initial attempts to heterologously express the SrpABC efflux pump in *Escherichia coli* enabled the instigation of solvent tolerance and production of 1-naphthol (15, 16). Importantly, the SrpABC efflux pump is encoded on the megaplasmid pTTS12 of *P. putida* S12 (12).

The 583-kbp megaplasmid pTTS12 is a stable single-copy plasmid specific to *P. putida* S12 (12). It harbors several important operons and gene clusters enabling *P. putida* S12 to tolerate, resist, and survive the presence of various toxic compounds or otherwise harsh environmental conditions. Several examples include the presence of a complete styrene degradation pathway gene cluster, the RND efflux pump specialized for organic solvents (SrpABC), and several gene clusters conferring heavy metal resistance (12, 17, 18). In addition, through analysis using TADB2.0, a toxin-antitoxin database (19, 20), pTTS12 is predicted to contain three toxin-antitoxin modules. Toxin-antitoxin modules recently have been recognized as important determinants of resistance toward various stress conditions, like nutritional stress and exposure to sublethal concentration of chemical stressors (21, 22). Toxin-antitoxin modules identified in pTTS12 consist of an uncharacterized RPPX_26255-RPPX_26260 system and two identical copies of a VapBC system (23). RPPX_26255 and RPPX_26260 belong to a newly characterized type II toxin-antitoxin pair, COG5654-COG5642. While toxin-antitoxin systems are known to preserve plasmid stability through postsegregational killing of plasmid-free daughter cells (24), RPPX_26255-RPPX_26260 was also previously shown to be upregulated during organic solvent exposure, suggesting its role in solvent tolerance (11).

In the manuscript, we further address the role of pTTS12 in conferring solvent tolerance of *P. putida* S12. Curing pTTS12 from its host strain might cause a reduction in solvent tolerance, while complementation of the *srp* operon into the cured strain may fully or partially restore solvent tolerance. Furthermore, we wished to identify additional genes or gene clusters on pTTS12 and putative mechanisms that might also play a role in conferring solvent tolerance to *P. putida* and non-solvent-tolerant *E. coli*.

RESULTS

Megaplasmid pTTS12 is essential for solvent tolerance in *P. putida* S12. To further analyze the role of the megaplasmid of *P. putida* S12 in solvent tolerance, pTTS12 was removed from *P. putida* S12 using mitomycin C. This method was selected due to its reported effectiveness in removing plasmids from *Pseudomonas* sp. (25), although previous attempts regarded plasmids that were significantly smaller in size than pTTS12 (26). After treatment with mitomycin C (10 to 50 mg liter⁻¹), liquid cultures were plated on M9 minimal medium supplemented with indole to select for plasmid-cured colonies. Megaplasmid pTTS12 encodes two key enzymes, namely, styrene monooxygenase (SMO) and styrene oxide isomerase (SOI) that are responsible for the formation of indigo coloration from indole. This conversion results in indigo coloration in spot assays for wild-type *P. putida* S12, whereas white colonies are formed in the absence of megaplasmid pTTS12. With the removal of pTTS12, a loss of indigo coloration and, hence, of indigo conversion was observed in all three plasmid-cured strains and the negative control *P. putida* KT2440 (Fig. 1A).

With a mitomycin C concentration of 30 mg liter⁻¹, 2.4% (3 out of 122) of the obtained colonies appeared to be completely cured of the megaplasmid, underscoring the high genetic stability of the plasmid. No colonies survived the addition of 40 and 50 mg liter⁻¹ of mitomycin C, whereas all the colonies that survived the addition of 10 and 20 mg liter⁻¹ of mitomycin C retained the megaplasmid. Three independent

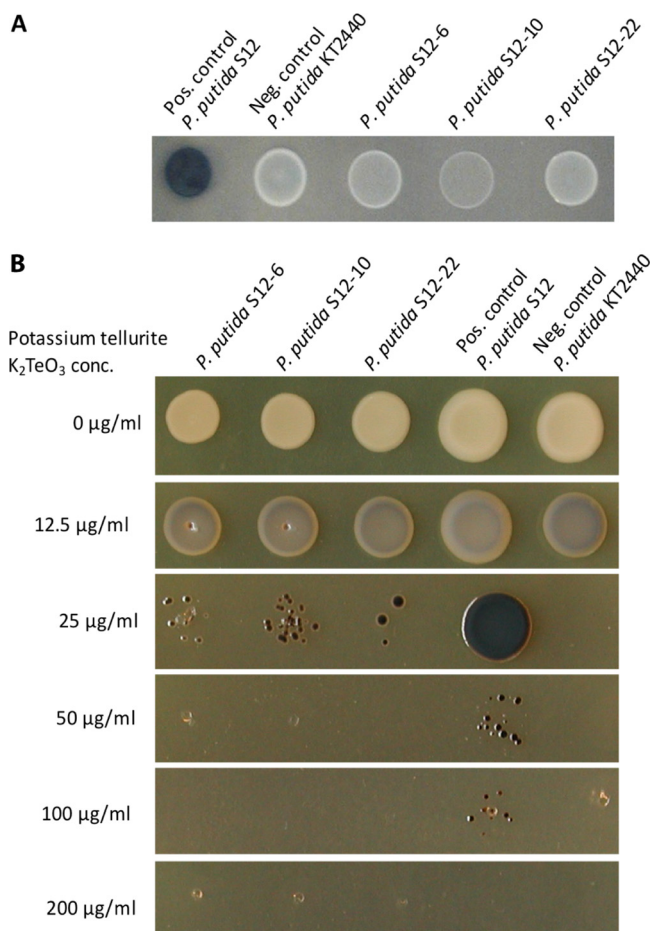


FIG 1 Curing of the megaplasmid pTTS12 from *P. putida* S12. (A) Activity of styrene monooxygenase (SMO) and styrene oxide isomerase (SOI) for indigo formation from indole in *P. putida* strains. Enzyme activity was lost in the megaplasmid-cured genotype S12 $\Delta pTTS12$ (white colonies). Indole ($100 \text{ mg liter}^{-1}$) was supplemented in M9 minimum medium. (B) K_2TeO_3 resistance of *P. putida* genotypes on lysogeny broth (LB) agar. Tellurite resistance was reduced in the megaplasmid-cured genotype S12 $\Delta pTTS12$ (MIC, 50 mg liter^{-1}).

colonies cured from the megaplasmid were isolated as *P. putida* S12-6, *P. putida* S12-10, and *P. putida* S12-22. The complete loss of the megaplasmid was further confirmed by phenotypic analysis (Fig. 1) and by full-genome sequencing. Several operons involved in heavy metal resistance were previously reported in the pTTS12 (12). The *terZABCD* operon contributes to tellurite resistance in wild-type *P. putida* S12 with MICs as high as $200 \text{ mg liter}^{-1}$ (Fig. 1B). In the megaplasmid-cured strains, a severe reduction of tellurite resistance was observed, decreasing the potassium tellurite MIC to 50 mg liter^{-1} (Fig. 1B).

Genomic DNA sequencing confirmed a complete loss of pTTS12 from *P. putida* genotypes S12-6, S12-10, and S12-22 without any plasmid-derived fragment being inserted within the chromosome, and genomic alterations by mitomycin C treatment were minimal. Complementation of pTTS12 into the plasmid-cured *P. putida* S12 genotypes restored the indole-indigo transformation and high tellurite resistance to a similar level as the wild-type strain (see Fig. S1 in the supplemental material). Repeated megaplasmid curing experiments indicated that *P. putida* S12 can survive the addition of 30 mg liter^{-1} mitomycin C with the frequency of $(2.48 \pm 0.58) \times 10^{-8}$. Among these survivors, only 2% of the colony population lost the megaplasmid, confirming the genetic stability of pTTS12. In addition, attempts to cure the plasmid by introducing double-strand breaks as described by Wynands and colleagues (27) were not successful due to the pTTS12 stability.

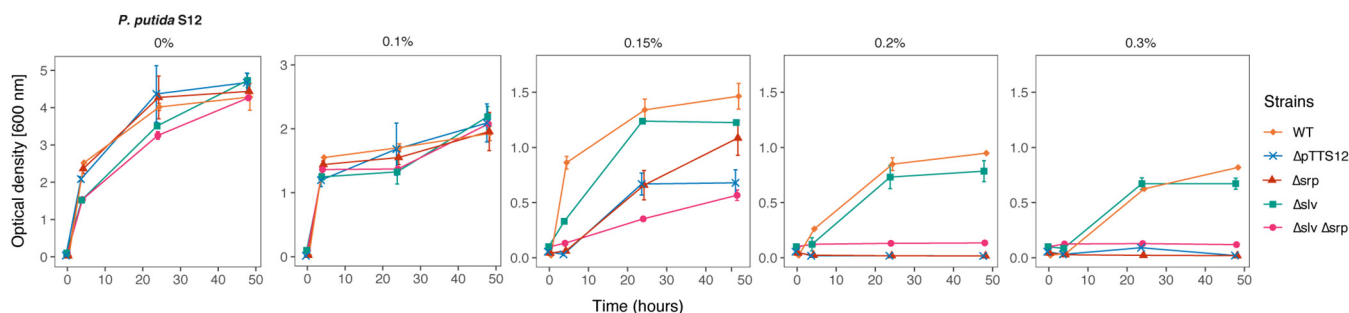


FIG 2 Megaplasmid pTTS12 determines the solvent tolerance trait of *P. putida* S12. Solvent tolerance analysis was performed on wild-type *P. putida* S12, *P. putida* S12 Δ pTTS12 (genotypes S12-6, S12-10, and S12-22), *P. putida* S12 Δ srp, *P. putida* S12 Δ slv, and *P. putida* S12 Δ srp Δ slv growing in liquid LB media with 0%, 0.10%, 0.15%, 0.20%, and 0.30% (vol/vol) toluene. The removal of the megaplasmid pTTS12 clearly caused a significant reduction in the solvent tolerance of *P. putida* S12 Δ pTTS12. Deletion of srpABC (Δ srp), RPPX_26255-RPPX_26260 (Δ slv), and the combination of these gene clusters (Δ srp Δ slv) resulted in a lower solvent tolerance. This figure displays the means of three biological replicates, and error bars indicate standard deviation. The ranges of the y axes are different in the first panel (0 to 5), second panel (0 to 3), and third to fifth panels (0 to 1.5).

Growth comparison in solid and liquid culture in the presence of toluene was performed to analyze the effect of megaplasmid curing in constituting the solvent tolerance trait of *P. putida* S12. In contrast with wild-type *P. putida* S12, the plasmid-cured genotypes were unable to grow under toluene atmosphere conditions (data not shown). In liquid LB medium, plasmid-cured *P. putida* S12 genotypes were able to tolerate 0.15% (vol/vol) toluene, whereas the wild-type *P. putida* S12 could grow in the presence of 0.30% (vol/vol) toluene (Fig. 2). In the megaplasmid-complemented *P. putida* S12-C genotypes, solvent tolerance was restored to the wild-type level (Fig. S1D). Hence, the absence of megaplasmid pTTS12 caused a significant reduction of solvent tolerance in *P. putida* S12.

The SrpABC efflux pump and gene pair RPPX_26255-RPPX_26260 are the main constituents of solvent tolerance encoded on pTTS12. The significant reduction of solvent tolerance in plasmid-cured *P. putida* S12 underscored the important role of megaplasmid pTTS12 in solvent tolerance. Besides encoding the efflux pump SrpABC enabling efficient intermembrane solvent removal (12, 13), pTTS12 carries more than 600 genes and, hence, may contain additional genes involved in solvent tolerance. Two adjacent hypothetical genes, RPPX_26255 and RPPX_26260, were previously reported to be upregulated in a transcriptomic study as a short-term response to toluene addition (11). We propose to name the RPPX_26255-RPPX_26260 gene pair as “slv” due to its elevated expression in the presence of solvent. In a first attempt to identify additional potential solvent tolerance regions of pTTS12, we deleted the srpABC genes (Δ srp), RPPX_26255-RPPX_26260 genes (Δ slv), and the combination of both gene clusters (Δ srp Δ slv) from pTTS12 in wild-type *P. putida* S12.

All strains were compared for growth under increasing toluene concentrations in liquid LB medium (Fig. 2). In the presence of low concentrations of toluene (0.10% [vol/vol]), all genotypes showed similar growth. With the addition of 0.15% (vol/vol) toluene, S12 Δ slv, S12 Δ srp, and S12 Δ srp Δ slv exhibited slower growth and reached a lower optical density at 600 nm (OD_{600}) than the wild-type S12 strain. S12 Δ slv and S12 Δ srp achieved a higher OD_{600} in batch growth than S12 Δ pTTS12 and S12 Δ srp Δ slv due to the presence of the SrpABC efflux pump or RPPX_26255-RPPX_26260 gene pair.

Interestingly, S12 Δ srp Δ slv (still containing pTTS12) exhibited diminished growth compared with S12 Δ pTTS12. This may be an indication of megaplasmid burden in the absence of essential genes for solvent tolerance. With 0.20% and 0.30% (vol/vol) toluene added to the medium, S12 Δ srp, S12 Δ srp Δ slv, and S12 Δ pTTS12 were unable to grow, while wild-type S12 and S12 Δ slv were able to grow, although S12 Δ slv reached a lower OD_{600} . Taken together, these results demonstrate an important role for both the SrpABC efflux pump and the slv gene pair in conferring solvent tolerance. We chose *P. putida* S12-6 for further experiments representing megaplasmid-cured *P. putida* S12.

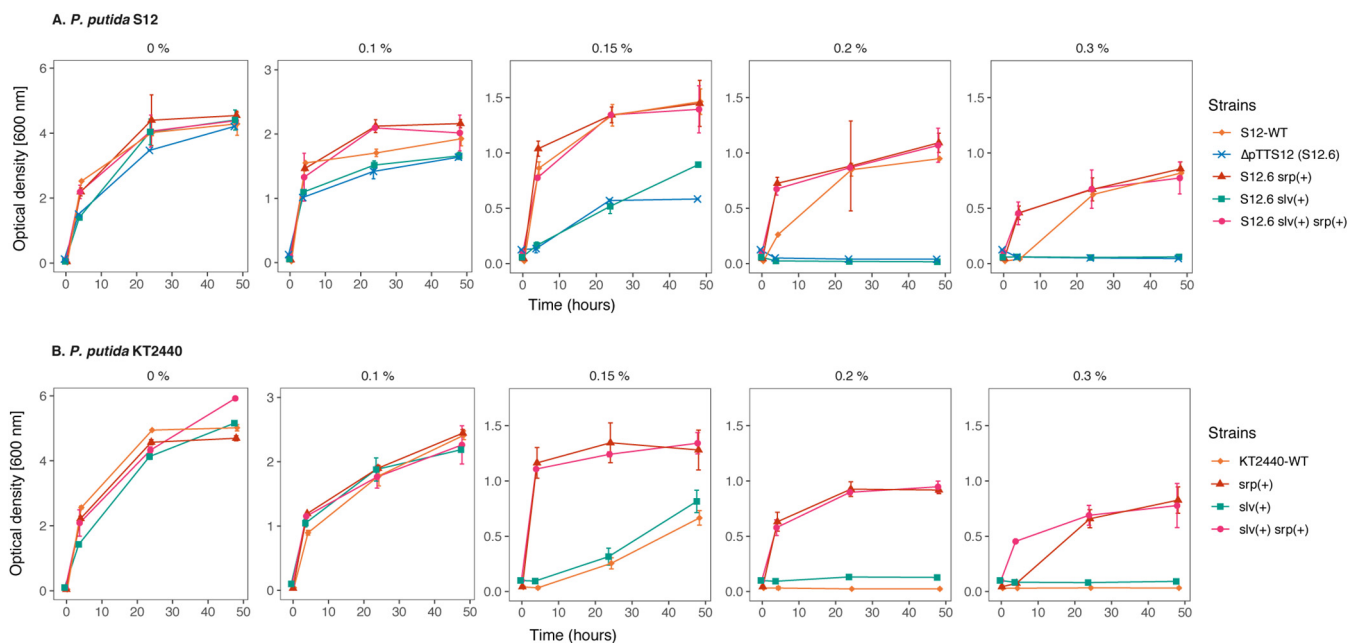


FIG 3 Chromosomal introduction of *srp* and *slv* gene clusters increased solvent tolerance in *P. putida* genotypes. Solvent tolerance analysis of the genotypes with chromosomal introduction of *srp* operon (*srpRSABC*), *slv* gene pair (RPPX_26255-RPPX_26260), and the combination of these gene clusters into *P. putida* S12 Δ pTTS12 (represented by strain S12-6) (A) and wild-type *P. putida* KT2440 (B) in liquid LB with 0%, 0.10%, 0.15%, 0.20%, and 0.30% (vol/vol) of toluene. Wild-type *P. putida* S12 was taken as a solvent-tolerant control strain. This figure displays the mean of three independent replicates, and error bars indicate standard deviation. The ranges of y axes are different in the first panel (0 to 6), second panel (0 to 3), and third to fifth panels (0 to 1.5).

Solvent tolerance can be exerted by ectopic expression of the *SrpABC* efflux pump and *slv* gene pair in Gram-negative bacteria.

The functionality of the *srp* operon and *slv* gene pair was explored in the model Gram-negative non-solvent-tolerant strains *P. putida* KT2440, *E. coli* TG1, and *E. coli* BL21(DE3). We complemented *srpRSABC* (*srp* operon), *slv* gene pair, and a combination of both gene clusters into *P. putida* S12-6, *P. putida* KT2440, *E. coli* TG1, and *E. coli* BL21(DE3) using mini-Tn7 transposition. These strains were chosen due to their common application as model industrial strains while lacking solvent tolerance. *P. putida* KT2440 is another robust microbial host for metabolic engineering due to its adaptation toward physicochemical stresses; however, contrary to *P. putida* S12, this strain is not solvent tolerant (28). *E. coli* BL21(DE3), derived from strain B, is the common *E. coli* lab strain optimized for protein production due to its lacking Lon and OmpT proteases and encoding T7 RNA polymerase (29). *E. coli* TG1 was previously reported to successfully produce 1-naphthol with the expression of *SrpABC* (15, 16), and therefore, this strain was included in this study as a comparison.

The chromosomal introduction of *slv* into S12-6 and KT2440 improved the growth of the resulting strains at 0.15% (vol/vol) toluene compared with S12-6 and KT2440 (Fig. 3). The introduction of *srp* or a combination of *slv* and *srp* enables S12-6 and KT2440 to grow in the presence of 0.30% (vol/vol) toluene. In KT2440, the introduction of both *slv* and *srp* resulted in a faster growth in the presence of 0.30% (vol/vol) toluene than the addition of only *srp* (Fig. 3B). Interestingly, the growth of S12-6 *srp,slv* and S12.6 *srp* is better than wild-type S12 (Fig. 3A). The observed faster growth of S12-6 *srp,slv* and S12.6 *srp* may be due to more efficient growth in the presence of toluene, supported by a chromosomally introduced *srp* operon, than its original megaplasmid localization. Indeed, replication of this large megaplasmid is likely to require additional maintenance energy. To corroborate this, we complemented the megaplasmid pTTS12 lacking the solvent pump ($Tc^r::srpABC$) into *P. putida* S12-6 *srp*, resulting in *P. putida* S12-9. Indeed, *P. putida* S12-9 showed further reduced growth in the presence of 0.20 and 0.30% toluene (see Fig. S2 in the supplemental material), indicating the metabolic burden of

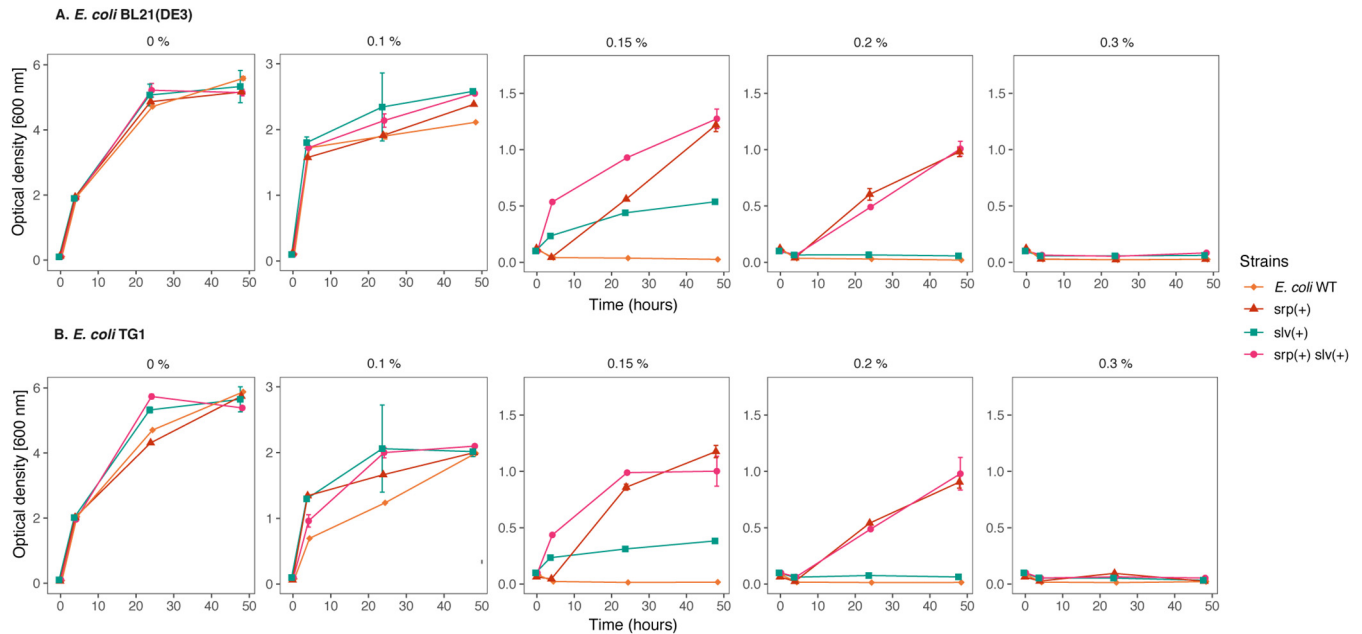


FIG 4 Chromosomal introduction of *srp* and *slv* gene clusters increased solvent tolerance in *E. coli* strains. Solvent tolerance analysis of the strains with chromosomal introduction of *srp* operon (*srpRSABC*), *slv* gene pair (RPPX_26255-RPPX_26260), and the combination of these gene clusters into *E. coli* BL21(DE3) (A) and *E. coli* TG1 (B) in liquid LB with 0%, 0.10%, 0.15%, 0.20%, and 0.30% (vol/vol) of toluene. This figure displays the mean of three independent replicates, and error bars indicate standard deviation. The ranges of y axes are different in the first panel (0 to 6), second panel (0 to 3), and third to fifth panels (0 to 1.5).

carrying the megaplasmid. We conclude that the SrpABC efflux pump can be regarded as the major contributor to solvent tolerance from pTTS12. The *slv* gene pair appears to promote the tolerance of *P. putida* S12 at least under moderate solvent concentrations.

The intrinsic solvent tolerance of *E. coli* strains was observed to be clearly lower than that of *P. putida* (Fig. 4). The wild-type *E. coli* strains were able to withstand a maximum 0.10% (vol/vol) toluene, whereas plasmid-cured *P. putida* S12-6 and *P. putida* KT2440 were able to grow in the presence of 0.15% (vol/vol) toluene. With the introduction of *slv* and *srp* in both *E. coli* strains, solvent tolerance was increased up to 0.15% and 0.20% (vol/vol) toluene, respectively (Fig. 4). A combination of *slv* and *srp* also increased tolerance to 0.20% (vol/vol) toluene, while showing a better growth than the chromosomal introduction of only *srp*. However, none of these strains were able to grow in the presence of 0.30% (vol/vol) toluene.

qPCR analysis of SrpABC expression (see Table S1 in the supplemental material) in *P. putida* S12, *P. putida* KT2440, *E. coli* TG1, and *E. coli* BL21(DE3) confirmed that *srpA*, *srpB*, and *srpC* were expressed at basal levels in all strains. In the presence of 0.10% toluene, the expression of *srpA*, *srpB*, and *srpC* was clearly upregulated in all strains. Thus, the lower solvent tolerance conferred by introducing the SrpABC efflux pump in *E. coli* strains was not due to the lower expression of the *srp* genes. An analysis of the codon adaptation index (CAI) (<http://ppuigbo.me/programs/CAIcal/>) (30) showed that for both the *P. putida* and *E. coli* strains, the CAI values of the *srp* operon are suboptimal, clearly below 0.8 to 1.0 (see Table S2 in the supplemental material). Interestingly, the CAI values were higher for *E. coli* (0.664) than for *P. putida* (0.465), predicting a better protein translation efficiency of the *srp* operon in *E. coli*. Hence, reduced translation efficiency is not likely to be the cause of lower performance of the *srp* operon in *E. coli* strains for generating solvent tolerance. Overall, our results indicate that, in addition to the solvent efflux pump, *P. putida* S12 and *P. putida* KT2440 are intrinsically more robust than *E. coli* TG1 and *E. coli* BL21(DE3) in the presence of toluene.

The *slv* gene pair constitutes a novel toxin-antitoxin system. BLASTp analysis was initiated to further characterize RPPX_26255 and RPPX_26260. This analysis indi-

cated that RPPX_26260 and RPPX_26255 likely represent a novel toxin-antitoxin (TA) system. Through a database search on TADB2.0 (19, 20), we found that RPPX_26260 is a toxin of the COG5654 family and typically carries an RES domain-containing protein, which has a conserved arginine (R)-glutamine (E)-serine (S) motif providing a putative active site; and RPPX_26255 is an antitoxin of the COG5642 family. Based on its involvement in solvent tolerance, we propose naming the toxin-encoding RPPX_26260 as *slvT* and the antitoxin-encoding RPPX_26255 as *slvA*.

Makarova and colleagues identified putative toxin-antitoxin pairs through genome mining of reference sequences in the NCBI database (31). They identified 169 pairs of the COG5654-COG5642 TA system from the reference sequences. Here, we constructed a phylogenetic tree of the COG5654-COG5642 TA system, including SlvA (GenBank accession no. [AJA16859.1](#)) and SlvT ([AJA16860.1](#)), as shown in Fig. 5A and 6A. SlvA and SlvT cluster with other plasmid-borne toxin-antitoxin from *Burkholderia vietnamensis* G4, *Methylbium petroleiphilum* PM1, *Rhodospirillum rubrum* ATCC 11170, *Xanthobacter autotrophicus* Py2, *Sinorhizobium meliloti* 1021, *Sinorhizobium medicae* WSM419, and *Gloeobacter violaceus* PCC7421. Multiple alignments of SlvAT against the COG5654-COG5642 TA system are shown in Fig. 5B and 6B.

Of the 169 TA pairs of the COG5654-COG5642 TA system, three TA pairs have recently been characterized, namely, ParST from *Sphingobium* sp. YBL2 (GenBank accession no. [AJR25281.1](#) and [AJR25280.1](#)) (32), PP_2433-PP_2434 from *P. putida* KT2440 ([NP_744581.1](#) and [NP_744582.1](#)) (33), and MbcAT from *Mycobacterium tuberculosis* H37Rv ([NP_216506.1](#) and [NP_216505.1](#)) (34), as indicated by bold text and asterisks in Fig. 5A and 6A. A 3D-model prediction of the SlvT and SlvA proteins using the I-TASSER suite for protein structure and function prediction (35) indicated that SlvT and SlvA showed the highest structural similarity to the MbcAT system from *Mycobacterium tuberculosis* (Fig. 5C and 6C), which is reported to be expressed during stress conditions (34). Amino acid conservation between SlvAT and these few characterized toxin-antitoxin pairs is relatively low, as they do not belong to the same clade (Fig. 5A and 6A). However, 100% conservation is clearly observed on the putative active side residues, namely, arginine (R) 35, tyrosine (Y) 45, and glutamine (E) 56, and only 75% consensus is shown on serine (S) 133 residue (see Fig. S3 in the supplemental material).

According to the model with the highest TM score, SlvT is predicted to consist of four beta sheets and four alpha helices. As such, SlvT shows structural similarity with diphtheria toxin which functions as an ADP-ribosyl transferase enzyme. Diphtheria toxin can degrade NAD⁺ into nicotinamide and ADP ribose (36). A similar function was recently identified for COG5654 family toxins from *P. putida* KT2440, *M. tuberculosis*, and *Sphingobium* sp. (32–34).

***slvT* toxin causes cell growth arrest by depleting cellular NAD⁺.** To prove that *slvAT* presents a pair of toxin and antitoxin, *slvA* and *slvT* were cloned separately in pUK21 (lac-inducible promoter) and pBAD18 (ara-inducible promoter), respectively. The two constructs were cloned into *E. coli* BL21(DE3). The growth of the resulting strains was monitored during conditional expression of the *slvA* and *slvT* genes (Fig. 7A). At the mid-log growth phase, a final concentration of 0.8% arabinose was added to the culture (*), inducing expression of *slvT*. After 2 h of induction, growth of this strain ceased, while the uninduced control culture continued to grow. Upon addition of 2 mM isopropyl- β -D-thiogalactopyranoside (IPTG) (**), growth of the *slvT*-induced culture was immediately restored, reaching a similar OD₆₀₀ as the uninduced culture.

Bacterial cell division was further studied by flow cytometer analyses during the expression of *slvT* and *slvA*. After approximately 6 h of growth (indicated by gray arrow in Fig. 7A), samples were taken from control, arabinose, and arabinose + IPTG-induced liquid culture. Cell morphology was analyzed by light microscopy, and the DNA content of the individual cells in the culture was measured using a flow cytometer with SYBR green II staining (Fig. 7B). Indeed, an absence of dividing cells and lower DNA content were observed during the induction of only *slvT* toxin with arabinose (Fig. 7B). Subsequent addition of IPTG to induce *slvA* expression was shown to restore cell division and

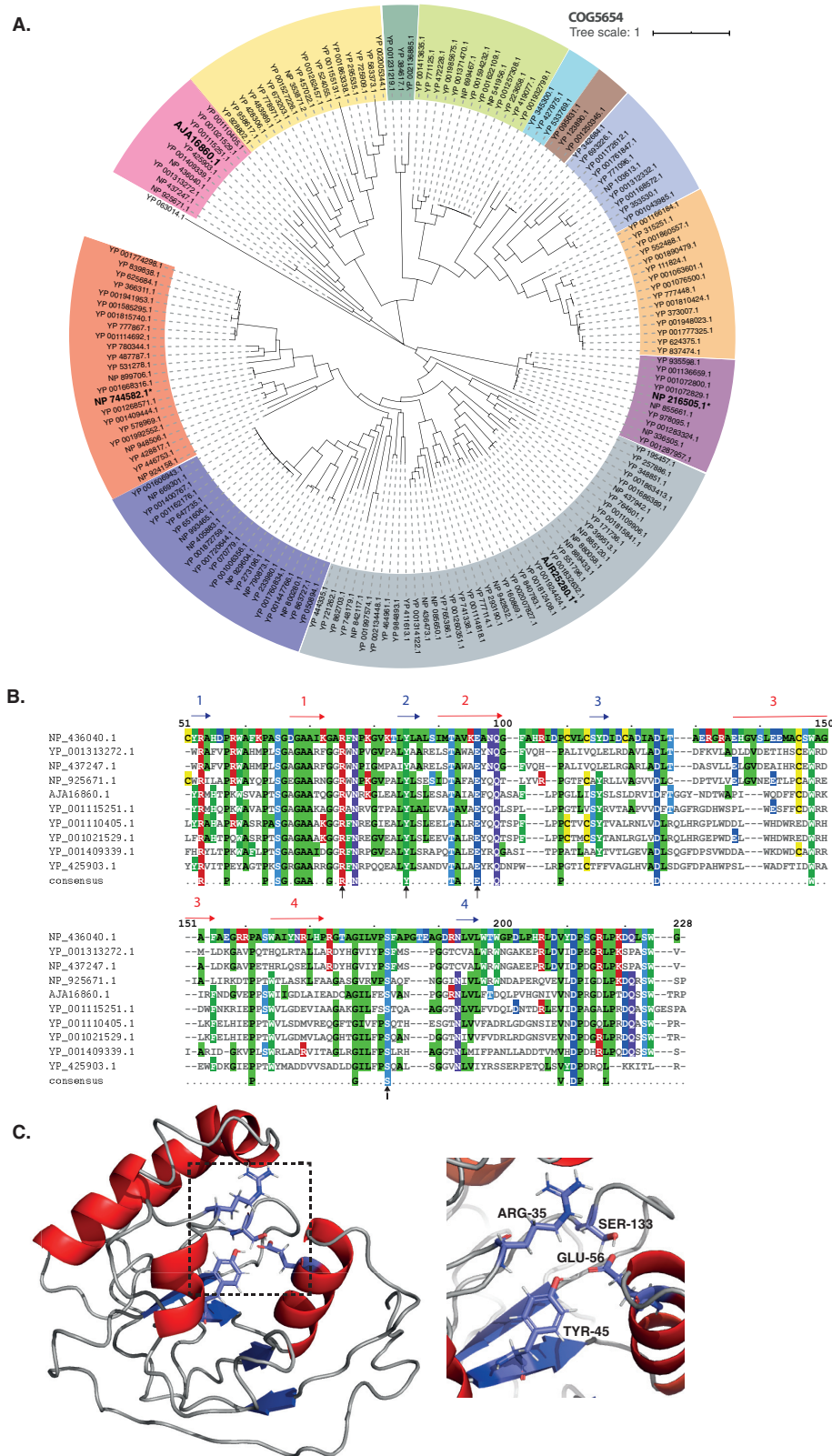


FIG 5 Bioinformatics analysis of SlvT as a member of the COG5654 toxin family. (A) Phylogenetic tree (neighbor-joining tree with 100 bootstraps) of COG5654 family toxin from reference sequences identified by Makarova and colleagues (31). Different colors correspond to the different toxin-antitoxin module clades. Asterisks (*) and bold text indicate the characterized toxin proteins, namely, ParT from *Sphingobium* sp. YBL2 (GenBank accession no. [AJR25280.1](https://www.ncbi.nlm.nih.gov/nuccore/AJ25280.1)), PP_2434 from *P. putida* KT2440 ([NP_744582.1](https://www.ncbi.nlm.nih.gov/nuccore/NP_744582.1)), MbcT from *Mycobacte-*

(Continued on next page)

to an upshift of DNA content similar to that of control strain (Fig. 7B). While the expression of *slvT* was not observed to be lethal to the bacterial strain, this experiment showed that the expression of the *slvT* toxin stalled DNA replication and, subsequently, cell division. The induction of *slvA* subsequently restored bacterial DNA replication and cell division.

To corroborate a putative target of *SlvT*, concentrations of NAD^+ were measured during the induction experiment (Fig. 7C). Before the addition of arabinose to induce *slvT* (orange arrow on Fig. 7A), NAD^+ was measured and compared to the strain harboring empty pUK21 and pBAD18 (Fig. 7B). On average, at this time point, the NAD^+ level is similar between the *slvAT*-bearing strain and the control strain. NAD^+ was measured again after arabinose induction when the growth of the induced strain has diminished (blue arrow on Fig. 7A). At this time point, the measured NAD^+ was 32% ($\pm 14.47\%$) of the control strain. After the induction of *slvA*, NAD^+ was immediately restored to a level of 77% ($\pm 9.97\%$) compared with the control strain. Thus, the induction of *slvT* caused a depletion of NAD^+ , while induction of *slvA* immediately increased the NAD^+ level, indicating that *slvAT* is a pair of toxin-antitoxin which controls its toxicity through NAD^+ depletion.

***slvAT* regulates megaplasmid pTTS12 stability.** In addition to its role in solvent tolerance, localization of the *slvAT* pair on megaplasmid pTTS12 may have an implications for plasmid stability. pTTS12 is a very stable megaplasmid that cannot be spontaneously cured from *P. putida* S12 and cannot be removed by introducing double-strand breaks (see above). We deleted *slvT* and *slvAT* from the megaplasmid to study their impact on pTTS12 stability. With the deletion of *slvT* and *slvAT*, the survival rate during treatment with mitomycin C improved significantly, reaching $(1.01 \pm 0.17) \times 10^{-4}$ and $(1.25 \pm 0.81) \times 10^{-4}$, respectively, while the wild-type S12 had a survival rate of $(2.48 \pm 0.58) \times 10^{-8}$.

We determined the curing rate of pTTS12 from the surviving colonies. In wild-type S12, the curing rate was 2% (see also above), while in $\Delta slvT$ and $\Delta slvAT$ mutants, the curing rate increased to 41.3% ($\pm 4.1\%$) and 79.3% ($\pm 10\%$), respectively, underscoring an important role for *slvAT* in megaplasmid stability. We attempted to cure the megaplasmid from the colonies by introducing a double-strand break (DSB), as previously described on *Pseudomonas taiwanensis* VLB120 (27, 37). This indeed was not possible in wild-type S12 and $\Delta slvT$ strains; however, the $\Delta slvAT$ mutant now showed plasmid curing by a DSB, resulting in a curing rate of 34.3% ($\pm 16.4\%$).

Since $\Delta slvT$ and $\Delta slvAT$ may compromise megaplasmid stability, we performed megaplasmid stability tests by growing S12 and KT2440 harboring pSW-2 (negative control) (37), pTTS12 (positive control), pTTS12 $\Delta slvT$, and pTTS12 $\Delta slvAT$ in LB medium with 10 passages (± 10 generations/passage step) as shown in Fig. 8. Both KT2440 and S12 easily lost the negative-control plasmid pSW-2 (Fig. 8). Plasmid pTTS12 was not lost during this test, confirming that pTTS12 is indeed a stable plasmid. Furthermore, the $\Delta slvT$ genotypes also did not show a loss of the megaplasmid. Interestingly, the $\Delta slvAT$ genotypes spontaneously lost the megaplasmid, confirming that the *slvAT* module is not only important to promote solvent tolerance but also determines megaplasmid stability in *P. putida* S12 and KT2440.

DISCUSSION

Revisiting the role of pTTS12 and the SrpABC efflux pump in solvent tolerance.

In this study, we conclusively confirm the role of the SrpABC efflux pump carried on pTTS12 and identify a novel toxin-antitoxin module playing an additional role in

FIG 5 Legend (Continued)

rium tuberculosis H37Rv (NP_216505.1), and *SlvT* from *P. putida* S12 (AJA16860.1). (B) Multiple sequence alignment of the COG5654 toxin *SlvT* from *P. putida* S12 with several putative COG5654 family toxin proteins which belong in the same clade. Putative active site residues are indicated by black arrows. (C) Protein structure modeling of *SlvT* using the I-TASSER server (35), which exhibits high structural similarity with MbcT from *Mycobacterium tuberculosis* H37Rv. Shown are the close ups of putative active sites of the *SlvT* toxin (Arg-35, Tyr-45, Glu-56, and Ser-133).

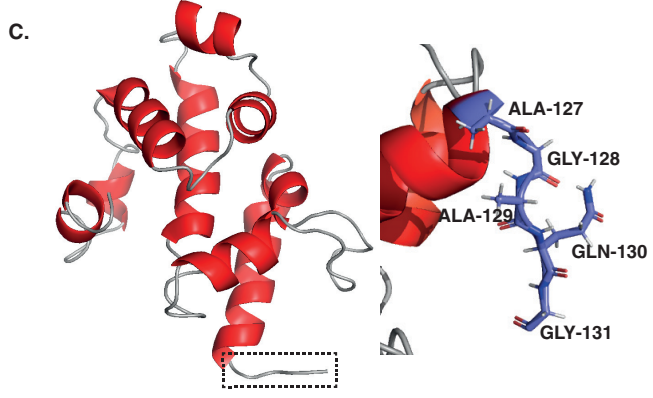
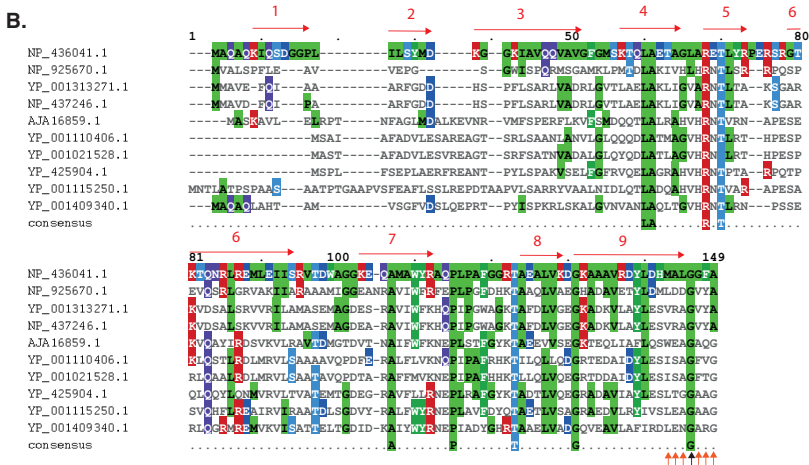
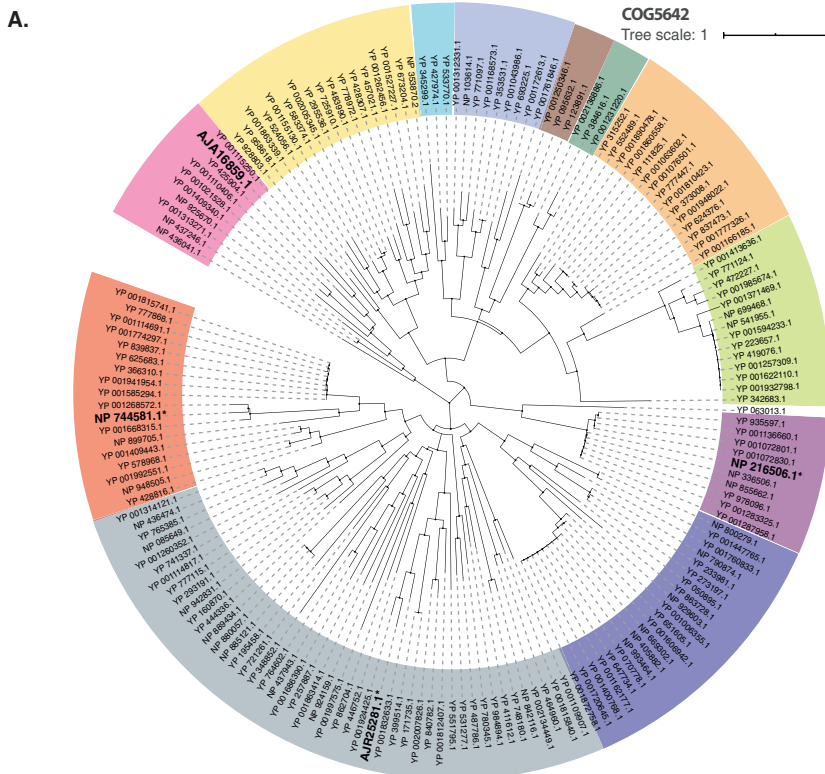


FIG 6 Bioinformatics analysis of SlvA as a member of the COG5642 toxin family. (A) Phylogenetic tree (neighbor-joining tree with 100 bootstraps) of the COG5642 family toxin from reference sequences identified by Makarova and colleagues (31). Different colors correspond to the different toxin-antitoxin (Continued on next page)

Downloaded from <http://aem.asm.org/> on June 17, 2020 by guest

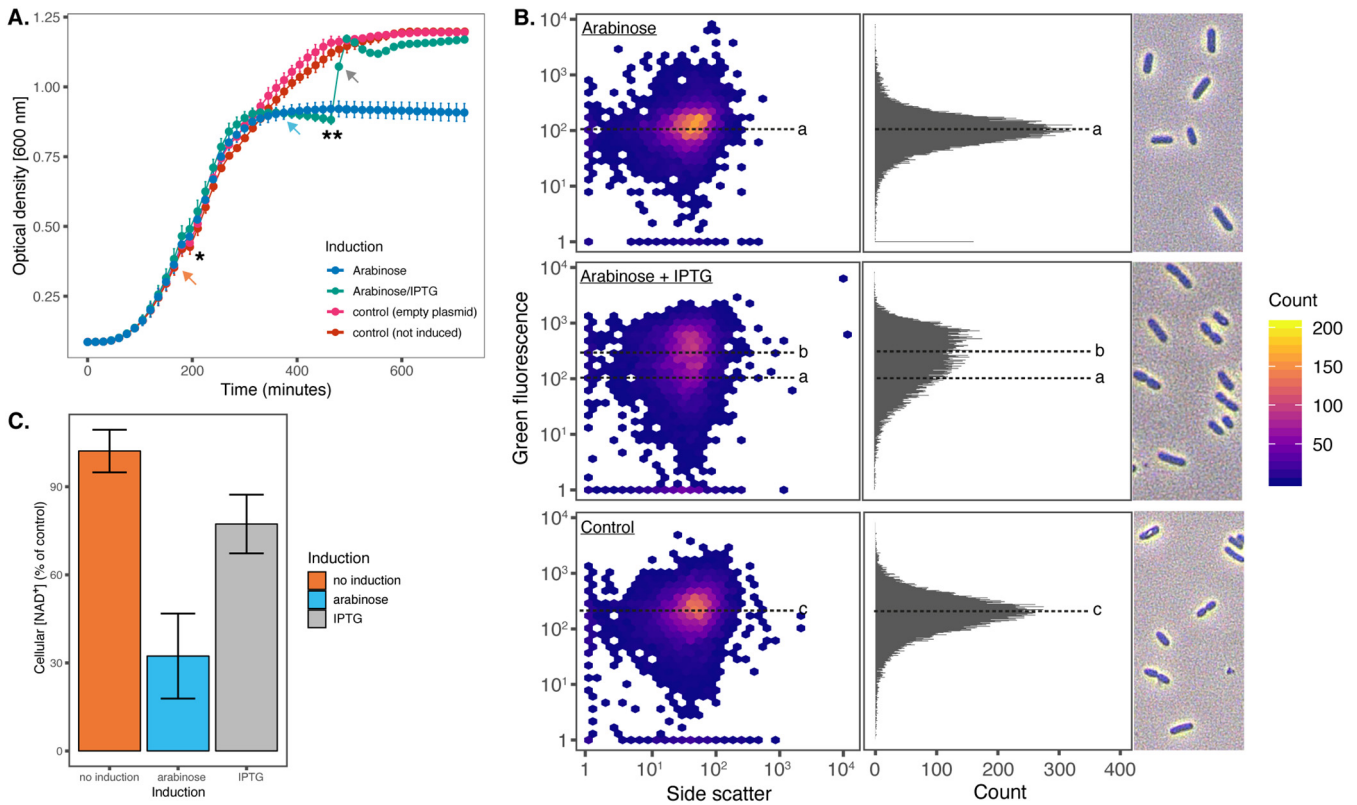


FIG 7 Heterologous expression of SlvAT in *E. coli* BL21(DE3). (A) Growth curves of *E. coli* BL21(DE3) harboring pBAD18-slvT and pUK21-slvA, showing growth reduction after the induction of toxin by a total concentration of 0.8% arabinose (*) and growth restoration after antitoxin induction by a total concentration of 2 mM IPTG (**). Samples were taken at the time points indicated by colored arrows for cellular NAD⁺ measurement. (B) Flow cytometry analysis of DNA content and cell morphology visualization on *E. coli* BL21(DE3) during *slvT* and *slvAT* expression. Median value of green fluorescence representing DNA content during *slvT* expression (118.202), *slvAT* expression (236.056), and control (208.406) are indicated by a, b, and c, respectively. Samples were taken at the time point indicated by the gray arrow in A. (C) Cellular NAD⁺ measurements during the expression of the toxin-antitoxin module. Induction of toxin SlvT caused a reduction in cellular NAD⁺ levels to 32.32% (\pm 14.47%) of the control strain, while the expression of SlvA restored the cellular NAD⁺ level to 77.27% (\pm 9.97%) of the control strain.

conveying solvent tolerance to *P. putida* S12 (Fig. 9). Notably, megaplasmids may cause a metabolic burden to their host strains, and they can be a source of genetic instability (11). Our results show that, indeed, pTTS12 imposed a metabolic burden in the presence of an organic solvent (Fig. S2). This plasmid is very large and contains many genes that are not related to solvent tolerance. Hence, it may be interesting for biotechnological purposes to reduce the plasmid size and, consequently, the metabolic burden. In addition, a streamlined and minimal genome size is desirable for reducing host interference and genome complexity (12, 13).

We investigated the heterologous expression of the SrpABC efflux pump in strains of both *P. putida* and *E. coli*, which successfully enhanced their solvent tolerance in these strains (Fig. 3 and 4). Previous reports on the implementation of SrpABC in whole-cell biocatalysis successfully increased the production of 1-naphthol in *E. coli* TG1 (15, 16). Production was still higher using *P. putida* S12, as this strain could better cope

FIG 6 Legend (Continued)

module clades. Asterisks (*) and bold text indicate the characterized toxin proteins, namely, ParS from *Sphingobium* sp. YBL2 (GenBank accession no. [AJR25281.1](https://www.ncbi.nlm.nih.gov/nuccore/AJR25281.1)), PP_2433 from *P. putida* KT2440 ([NP_744581.1](https://www.ncbi.nlm.nih.gov/nuccore/NP_744581.1)), MbcA from *Mycobacterium tuberculosis* H37Rv ([NP_216506.1](https://www.ncbi.nlm.nih.gov/nuccore/NP_216506.1)), and SlvA from *P. putida* S12 ([AJA16859.1](https://www.ncbi.nlm.nih.gov/nuccore/AJA16859.1)). (B) Multiple sequence alignment of the COG5654 toxin SlvA from *P. putida* S12 with several putative COG5642 family toxin proteins which belong in the same clade. Putative active site residues are indicated by orange and black arrows. (C) Protein structure modeling of SlvA using the I-TASSER server (35), which exhibits high structural similarity with MbcA from *Mycobacterium tuberculosis* H37Rv. Shown are the close ups of the antitoxin putative C-terminal binding site to block the SlvT toxin active site (Ala-127, Gly-128, Ala-129, Gln-130, and Gly-131).

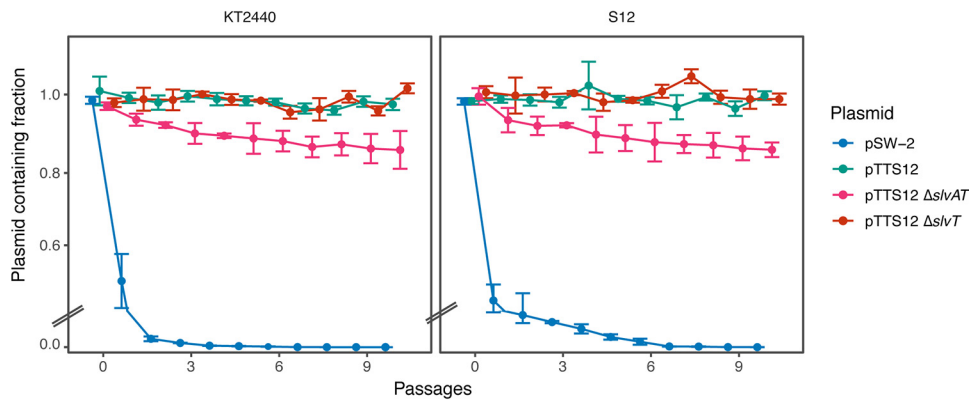


FIG 8 SlvAT is important for pTTS12 maintenance in *P. putida*. pTTS12 (variant with Km^r) maintenance in *P. putida* S12 and *P. putida* KT2440 growing in LB liquid medium without antibiotic selection for 10 passages (approximately 10 generations per passage). pSW-2 was taken as a negative control for plasmid stability in *P. putida*. This experiment was performed with three biological replicates, and error bars represent standard deviation.

with substrate (naphthalene) toxicity, while both *P. putida* S12 and *E. coli* TG1 showed similar tolerance to the product 1-naphthol (16). In our experiments, the *E. coli* strains clearly showed a smaller increase in toluene tolerance than the *P. putida* strains, although *srpABC* was expressed at a basal level and upregulated in the presence of 0.10% (vol/vol). These results indicate that besides having an efficient solvent efflux

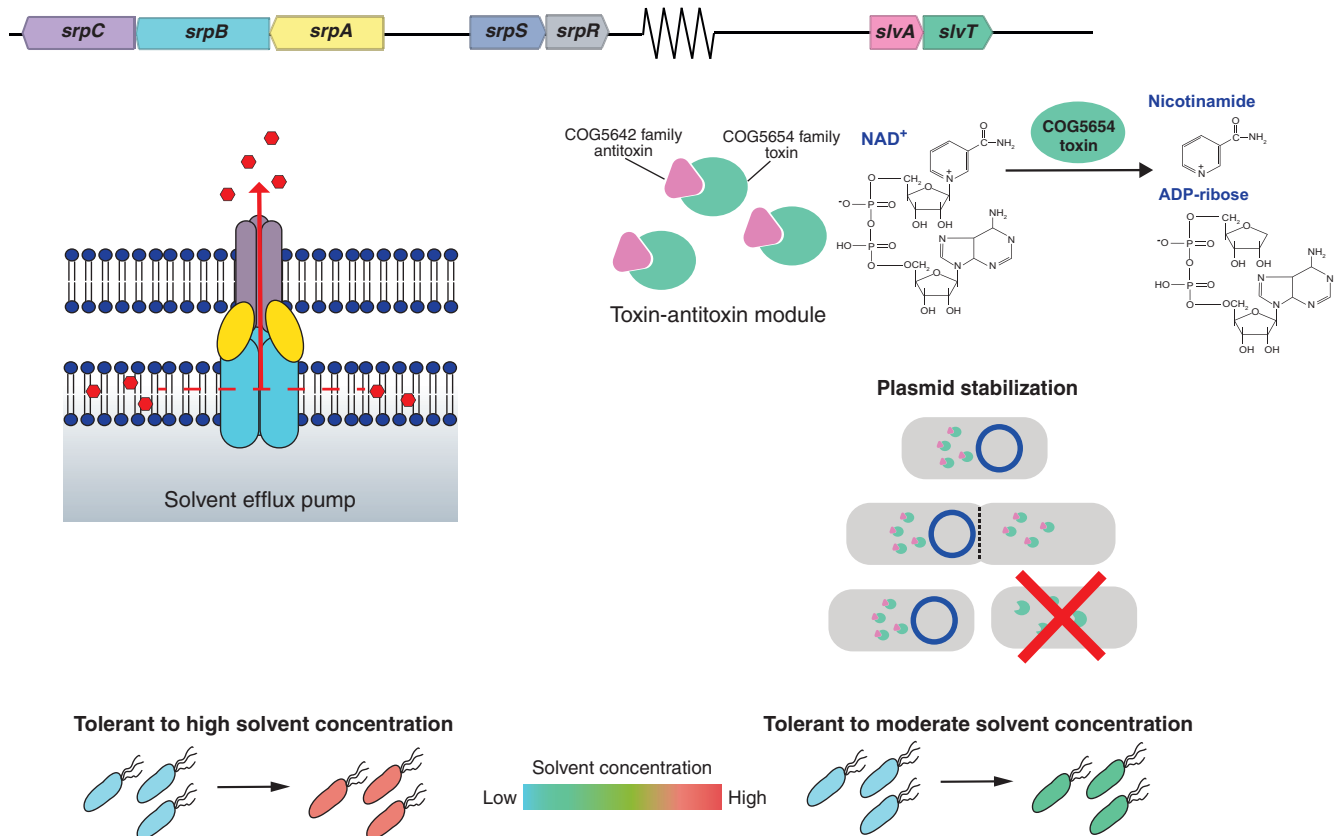


FIG 9 Schematic representation of the gene clusters involved in solvent tolerance from megaplasmid pTTS12. The *SrpABC* efflux pump is the major contributor to the solvent tolerance trait from the megaplasmid pTTS12. This efflux pump is able to efficiently extrude solvents from the membrane lipid bilayer. A COG5654-COG5642 family toxin-antitoxin module (*SlvT* and *SlvA*, respectively) promoted the growth of *P. putida* S12 in the presence of a moderate solvent concentration and stabilized the pTTS12 plasmid. In the absence of *SlvA*, *SlvT* causes toxicity by conferring cellular NAD⁺ depletion and, subsequently, halts DNA replication and cell division.

pump, *P. putida* S12 and *P. putida* KT2440 are inherently more robust in the presence of toluene and, presumably, other organic solvents than *E. coli* TG1 and *E. coli* BL21(DE3). The absence of *cis-trans* isomerase (*cti*), resulting in the inability to switch from *cis-* to *trans-*fatty acid in *E. coli* (38), may contribute to this difference in solvent tolerance. Additionally, *P. putida* typically has a high NAD(P)H regeneration capacity (39, 40) which can contribute to the maintenance of proton motive force during solvent extrusion by the RND efflux pump. Further detailed investigation is required to reveal the exact basis for its intrinsic robustness.

Identification of the novel antitoxin-toxin module SlvAT. In *P. putida* S12, deletion of *srpABC* genes still resulted in higher solvent tolerance than the pTTS12-cured genotypes (Fig. 2, panel 3). This finding indicated that within pTTS12 there were other gene(s) which may play a role in solvent tolerance. Two genes of unknown function were upregulated in a transcriptome analysis of toluene-shocked *P. putida*, namely, RPPX_26255 and RPPX_26260, suggesting a putative role in solvent tolerance (11). Here, we confirmed this finding and demonstrated that these genes together form a novel toxin-antitoxin module (Fig. 7). SlvT exerts toxicity by degradation of NAD⁺, like other toxins of the COG5654 family, and expression of antitoxin SlvA immediately restored NAD⁺ levels. Depletion of NAD⁺ interfered with DNA replication and caused an arrest of cell division similar to another recently described COG5654-COG5642 family toxin-antitoxin pair (33). Indeed, the SlvAT toxin-antitoxin module was shown to be important for the stability of pTTS12 (Fig. 8).

Based on TADB2.0 analysis, pTTS12 encodes three TA pairs, namely, SlvAT and two identical copies of VapBC. VapBC was first identified from a virulence plasmid of *Salmonella* sp. and is known to prevent the loss of plasmid during nutrient-limiting conditions (41). A previous report showed that VapBC can stabilize/retain approximately 90% of the pUC plasmid in *E. coli* within 300 h of growth (42), which is similar to our result although demonstrated in a much smaller plasmid and under the control of the lac operon. Serendipitous plasmid loss due to double-strand break was reported in pSTY, which carries two identical copies of VapBC (27). Here, we observed a similar phenomenon in pTTS12 Δ slvAT. Hence, in the absence of SlvAT, two copies of VapBC were not sufficient to prevent the loss of pTTS12 on rich media without selection pressure and by double-strand break, indicating a major role for SlvAT.

A putative role of toxin-antitoxin module SlvAT in solvent tolerance. Toxin-antitoxin modules are known to be important in antibiotic persistent strains as a trigger to enter and exit the dormant state, causing the cell to become unaffected by the antibiotic (42). Among *Pseudomonas* species, several toxin-antitoxin modules are reported to be involved in survival strategies, such as stress response, biofilm formation, and antimicrobial persistence (33, 43–45). Previous transcriptomic studies reported upregulation of the *slvAT* locus as a response toward toluene addition and its expression at 10 to 30 minutes after toluene addition (11). Here, we show that SlvAT improves solvent tolerance in *P. putida* and *E. coli* strains independent of pTTS12 or the SrpABC efflux pump. We hypothesize that SlvAT plays a role as a rapid response toward toluene addition. Activation of the SlvT toxin may halt bacterial growth, and this allows physiological adaptation and adjustments to take place (e.g., expression of extrusion pumps and membrane compaction) before resuming its growth and cell division in the presence of toxic organic solvent. It is interesting to note that *P. putida* S12 and KT2440 both carry another COG5654-COG5642 family toxin-antitoxin pair in their chromosome (locus tag RPPX_19375-RPPX_19380 and PP_2433-PP_2434, respectively). In *P. putida* S12, this TA module is not being induced during solvent stress, rendering it unlikely to play a role in solvent tolerance.

The putative regulation mechanism of toxin-antitoxin module SlvAT in *P. putida* S12. Expression of the *slvAT* locus with its native promoter region seemed to exert a similar physiological effect in solvent tolerance both in *E. coli* and *P. putida* (Fig. 3 and 4). Typically, toxin-antitoxin can regulate its own expression by antitoxin binding to the promoter region (46). Unstable antitoxin is encoded upstream of the stable toxin,

TABLE 1 Strains and plasmids used in this study

Strain, genotype, or plasmid	Characteristic(s)	Reference
Strain or genotype		
<i>P. putida</i>		
S12	Wild-type <i>P. putida</i> S12 (ATCC 700801), harboring megaplasmid pTTS12	3
S12-1	<i>P. putida</i> S12, harboring megaplasmid pTTS12 with Km ^r marker	This study
S12-6/S12-10/S12-22	ΔpTTS12	This study
S12-9	ΔpTTS12, Gm ^r <i>srpRSABC</i> ::Tn7, complemented with megaplasmid pTTS12 (Tc ^r :: <i>srpABC</i>)	This study
S12-C	<i>P. putida</i> ΔpTTS12 (S12-6/S12-10/S12-22), complemented with megaplasmid pTTS12	This study
KT2440	Derived from wild-type <i>P. putida</i> mt-2, ΔpWWO	46
<i>E. coli</i>		
HB101	<i>recA pro leu hsdR Sm^r</i>	47
BL21(DE3)	<i>E. coli</i> B, F ⁻ <i>ompT gal dcm lon hsdS_B(r_B⁻m_B⁻) λ(DE3) [lacI lacUV5-T7p07 ind1 sam7 nin5] [malB⁺]_{K-12}(λ^S)</i>	29
DH5α λpir	<i>sup E44, ΔlacU169 (ΦlacZΔM15), recA1, endA1, hsdR17, thi-1, gyrA96, relA1, λpir</i> phage lysogen	48
TG1	<i>E. coli</i> K-12, <i>glnV44 thi-1 Δ(lac-proAB) Δ(mcrB-hsdSM)5(r_K⁻m_K⁻) F'</i> [traD36 proAB ⁺ lac ^q lacZΔM15]	Lucigen
WM3064	<i>thrB1004 pro thi rpsL hsdS lacZΔM15 RP4-1360 Δ(araBAD)567 ΔdapA1341::[erm pir]</i>	William Metcalf
Plasmid		
pRK2013	RK2-Tra ⁺ , RK2-Mob ⁺ , Km ^r , ori ColE1	49
pEMG	Km ^r , Ap ^r , ori R6K, lacZα MCS flanked by two I-SceI sites	37
pEMG-Δ <i>srpABC</i>	pEMG plasmid for constructing <i>P. putida</i> S12 Δ <i>srpABC</i>	This study
pEMG-Δ <i>slvAT</i>	pEMG plasmid for constructing <i>P. putida</i> S12 Δ <i>slvAT</i>	This study
pEMG-Δ <i>slvT</i>	pEMG plasmid for constructing <i>P. putida</i> S12 Δ <i>slvT</i>	This study
pSW-2	Gm ^r , ori RK2, <i>xyIS</i> , Pm → I-SceI	37
pBG35	Km ^r , Gm ^r , ori R6K, pBG derived	44
pBG-srp	Km ^r , Gm ^r , ori R6K, pBG derived, contains <i>srp</i> operon (RPPX_27995-RPPX_27965)	This study
pBG-slv	Km ^r , Gm ^r , ori R6K, pBG derived, contains <i>slv</i> gene pair (RPPX_26255-RPPX_26260)	This study
pBG-srp-slv	Km ^r , Gm ^r , ori R6K, pBG derived, contains <i>slv</i> gene pair (RPPX_26255-RPPX_26260) and <i>srp</i> operon (RPPX_27995-RPPX_27965)	This study
pBAD18-slvT	Ap ^r , ara operon, contains <i>slvT</i> (RPPX_26260)	This study
pUK21-slvA	Km ^r , lac operon, contains <i>slvA</i> (RPPX_26255)	This study
pTnS-1	Ap ^r , ori R6K, TnSABC+D operon	50

giving a transcriptional advantage for the production of antitoxin (47). While this study presents a role of the SlvAT module as a response to solvent stress, this toxin-antitoxin module may play a role in the response to various other stresses since pTTS12 itself encodes several modules involved in different stress response. It would be interesting to further study whether organic solvents directly induce the expression of the *slvAT* locus or intermediate signaling pathways are required. Several type II toxin-antitoxin modules are known to be regulated by proteases, such as Lon and Clp (48). These proteases degrade the antitoxin protein, promoting toxin activity, and thus upregulate the expression of the toxin-antitoxin locus. Indeed, our preliminary transcriptomic data show upregulation of specific protease-encoding loci after toluene addition. They may constitute putative regulatory proteases to the SlvAT module. Future research on the dynamics of *slvAT* locus regulation is required for revealing the details of the control mechanisms operating *in vivo*.

Conclusions. In summary, our experiments confirmed that the SrpABC efflux pump is the major contributor of solvent tolerance on the megaplasmid pTTS12 which can be transferred to other non-solvent-tolerant host microbes. In addition, the megaplasmid carries the novel toxin-antitoxin system SlvAT (RPPX_26255 and RPPX_26260) which promotes rapid solvent tolerance in *P. putida* S12 and is important for maintaining the plasmid stability of pTTS12. Chromosomal introduction of the *srpRSABC* operon genes in combination with *slvAT* confers a clear solvent tolerance phenotype in other industrial strains previously lacking this phenotype, such as *P. putida* KT2440, *E. coli* TG1, and *E. coli* BL21(DE3). Taken together, our findings show that both SrpABC and SlvAT constitute suitable candidate loci for exchange with various microbial hosts for increasing tolerance toward toxic compounds.

MATERIALS AND METHODS

Strains and culture conditions. Strains and plasmids used in this study are listed in Table 1. All *P. putida* strains were grown in lysogeny broth (LB) at 30°C with 200 rpm shaking. *E. coli* strains were cultivated in LB at 37°C with 250 rpm shaking. For solid cultivation, 1.5% (wt/vol) agar was added to LB. M9 minimal medium was supplemented with 2 mg liter⁻¹ MgSO₄ and 0.2% of citrate as a sole carbon

TABLE 2 Primers used in this study

Primer	Sequence (5'–3')	Restriction site	PCR template	PCR description
TS1-srp-for	TATCTGGTACCTTGTCTGGAAGCCGCTAATGA	KpnI	pTTS12	Construction of pEMG- Δ srpABC
TS1-srp-rev	CAGCGGCGCCGCTTTAACGCAGGAAAGCTGCGAG	NotI	pTTS12	Construction of pEMG- Δ srpABC
TS2-srp-for	CCGAAGCGGCCGCCAGCGCAGTTAAGGGGATTACC	NotI	pTTS12	Construction of pEMG- Δ srpABC
TS2-srp-rev	TCAGCTCTAGAGCGCAGGTAAGGCTTCACC	XbaI	pTTS12	Construction of pEMG- Δ srpABC
srpO_F	TGCGAATTCGGTATCGCACATGGCATTGG	EcoRI	pTTS12	Construction of pBG-srp
srpO_R	TGCTCTAGAGCCTCACACCTGGGTGATACC	XbaI	pTTS12	Construction of pBG-srp
slv_F	ATGCTTAATTAACCTTTTGTCTGCGGTCTACACAGG	PacI	pTTS12	Construction of pBG-slv
slv_R	AGCGGGAATTCCTCCAAAACCGGTTCTGAAGCC	EcoRI	pTTS12	Construction of pBG-slv
slvA_F	AGAGAGCTCCATAGTAAGTGAATCCTAAAG	SacI	pTTS12	Construction of pUK21-slvA
slvA_R	GTCTAGACTCCAGCTCCAGATGTAG	XbaI	pTTS12	Construction of pUK21-slvA
slvT_F	GGTCTCTAGAATGAAAATCATCGGAGTG	XbaI	pTTS12	Construction of pBAD18-slvT
slvT_R	GGAAGGAGCTCGTACGTGAAGCGCTAC	SacI	pTTS12	Construction of pBAD18-slvT
TS1_slv_F	TGCTGGAATTCCTTTTGTCTGCGGTCTACACAGG	EcoRI	pTTS12	Construction of pEMG- Δ slvAT
TS1_slv_R	GGCAACTGATCGGTGAAAAGCACTTTGAGAGCGTCCATCAAGCC		pTTS12	Construction of pEMG- Δ slvAT
TS2_slv_F	GGCTTGATGGACGCTCTCAAAGTGCTTTTCACCGATCAGTTGC		pTTS12	Construction of pEMG- Δ slvAT
TS2_slv_R	GCCAGGATCCCAGATGTCCATAATCCAGGCGC	KpnI	pTTS12	Construction of pEMG- Δ slvAT
TS1_slvT_F	GCATAGGATCCGAGAATTGTGCATAGTAAGTG	KpnI	pTTS12	Construction of pEMG- Δ slvT
TS1_slvT_R	GATCGTTGACCACAATATCTCCAGCTCCAGATGTAG		pTTS12	Construction of pEMG- Δ slvT
TS2_slvT_F	CTACATCTGGAGCTGGAGATATTGTGGTCAACGATC		pTTS12	Construction of pEMG- Δ slvT
TS2_slvT_R	AGGTTAAGCTTGTCTGCAAGTGTCTTATCC	HindIII	pTTS12	Construction of pEMG- Δ slvT
eco_gyrB_F	CGATAATTTTGCCAAACCACGAT		<i>gyrB</i>	qPCR, reference gene
eco_gyrB_R	GAAATTCCTCCAGACCAAAA		<i>gyrB</i>	qPCR, reference gene
eco_rpoB_F	AACACGAGTTCGAGAAGAAAAT		<i>rpoB</i>	qPCR, reference gene
eco_rpoB_R	CGTTTAACCGCCAGATATACTT		<i>rpoB</i>	qPCR, reference gene
ppu_gyrB_F	GCTTCGACAAGATGATTTTCGTC		<i>gyrB</i>	qPCR, reference gene
ppu_gyrB_R	GCAGTTTGTGATGTTGACTC		<i>gyrB</i>	qPCR, reference gene
ppu_rpoB_F	GACAAGGAATCGTCAACAAAAG		<i>rpoB</i>	qPCR, reference gene
ppu_rpoB_R	GAAGGTACCGTTCAGTCATC		<i>rpoB</i>	qPCR, reference gene
srpA_F	CTCGAAAACCTCAGAGTTCCT		<i>srpA</i>	qPCR, target gene
srpA_R	AAAGCTTCTGGTCTGCAAAAAG		<i>srpA</i>	qPCR, target gene
srpB_F	TACATGACCAGGAAGACCAGTA		<i>srpB</i>	qPCR, target gene
srpB_R	GTGGAGGTCATTTATCCCTACG		<i>srpB</i>	qPCR, target gene
srpC_F	GCCATAAGTTGATGTTTCAGCAG		<i>srpC</i>	qPCR, target gene
srpC_R	ATTCCAACGGATTGCCCCAAA		<i>srpC</i>	qPCR, target gene

source (43). Toluene atmosphere growth was evaluated on solid LB in a glass plate incubated in an excicator with toluene supplied through the gas phase at 30°C. Solvent tolerance analysis was performed by growing *P. putida* S12 genotypes in LB starting from OD₆₀₀ of 0.1 in Boston bottles with Mininert bottle caps. When required, gentamicin (25 mg liter⁻¹), ampicillin (100 mg liter⁻¹), kanamycin (50 mg liter⁻¹), indole (100 g liter⁻¹), potassium tellurite (6.75 to 200 mg liter⁻¹), arabinose (0.8% m/v), and IPTG (2 mM) were added to the medium.

DNA and RNA methods. All PCRs were performed using Phusion polymerase (Thermo Fisher) according to the manufacturer's manual. Primers used in this study (Table 2) were procured from Sigma-Aldrich. PCR products were checked by gel electrophoresis on 1% (wt/vol) Tris-borate-EDTA (TBE) agarose containing 5 μ g ml⁻¹ ethidium bromide (110 V, 0.5 \times TBE running buffer). For reverse transcriptase quantitative PCR (RT-qPCR) analysis, RNA was extracted using TRIzol reagent (Invitrogen) according to the manufacturer's manual. The obtained RNA samples were immediately reverse transcribed using the iScript cDNA synthesis kit (Bio-Rad), and cDNA may have been stored at -20°C prior to qPCR analysis. qPCR was performed using iTaq universal SYBR green supermix (Bio-Rad) on a CFX96 Touch real-time PCR detection system (Bio-Rad). The genome sequence of *P. putida* S12 Δ pTTS12 was analyzed using an Illumina HiSeq instrument (GenomeScan BV, The Netherlands) and assembled according to the existing complete genome sequence (GenBank accession no. CP009974 and CP009975) (12).

Curing and complementation of megaplasmid pTTS12 from *P. putida* S12. *P. putida* S12 was grown in LB to reach early-exponential phase (approximately 3 h or OD₆₀₀ of 0.4 to 0.6). Subsequently, mitomycin C was added to the liquid LB culture to a final concentration of 10, 20, 30, 40, or 50 μ g/ml. These cultures were grown for 24 h and plated on M9 minimal medium supplemented with indole to select for the absence of the megaplasmid. Loss of the megaplasmid was confirmed by a loss of other phenotypes connected with the megaplasmid, such as MIC reduction of potassium tellurite and solvent sensitivity under toluene atmosphere, as well as through genomic DNA sequencing. Complementation of megaplasmid pTTS12 was performed using biparental mating between *P. putida* S12-1 (pTTS12 Km^r) and plasmid-cured genotype *P. putida* S12 Δ pTTS12 (Gm^r:Tn7) and followed by selection on LB agar supplemented with kanamycin and gentamicin.

Plasmid cloning. Deletion of *srpABC*, *slvT*, and *slvAT* genes was performed using homologous recombination between free-ended DNA sequences that are generated by cleavage at unique I-SceI sites (37). Two homologous recombination sites were chosen downstream (TS-1) and upstream (TS-2) of the target genes. TS-1 and TS-2 fragments were obtained by performing PCR using primers listed in Table S1.

Constructs were verified by DNA sequencing. Mating was performed as described by Wynands and colleagues (27). Deletion of *srpABC*, *slvT*, and *slvAT* was verified by PCR and Sanger sequencing (Macrogen B.V., Amsterdam, The Netherlands).

Introduction of the complete *srp* operon (*srpRSABC*) and *slvAT* was accomplished using the mini-Tn7 delivery vector backbone of pBG35 developed by Zobel and colleagues (44). The DNA fragments were obtained by PCR using primer pairs listed in Table 2 and ligated into the pBG35 plasmid at PacI and XbaI restriction sites. This construct generated a Tn7 transposon segment in pBG35 containing a gentamicin resistance marker and *srp* operon with Tn7 recognition sites flanking on the 5' and 3' sides of the segment. Restriction analysis followed by DNA sequencing (Macrogen, The Netherlands) were performed to confirm the correct pBG-srp, pBG-slv, and pBG-srp-slv construct. The resulting construct was cloned in *E. coli* WM3064 and introduced into *P. putida* or *E. coli* strains with the help of *E. coli* WM3064 pTnS-1. Integration of the construct into the Tn7 transposon segment was confirmed by gentamicin resistance, PCR, and the ability of the resulting transformants to withstand and grow under toluene atmosphere conditions.

Toxin-antitoxin assay. Bacterial growth during the toxin-antitoxin assay was observed in LB medium supplemented with 100 mg liter⁻¹ ampicillin and 50 mg liter⁻¹ kanamycin. Starting cultures were inoculated from a 1:100 dilution of overnight culture (OD₆₀₀, 0.1) into a microtiter plate (96 well), and bacterial growth was measured using a Tecan Spark 10M instrument. To induce toxin and antitoxin, a total concentration of 0.8% (m/vol) arabinose and 2 mM IPTG were added to the culture, respectively. Cell morphology was observed using a light microscope (Zeiss Axiolab 5) at a magnification of ×100. A final concentration of 2.5× SYBR green I (10,000× stock; New England BioLabs) was applied to visualize DNA, followed by two times washing with 1× phosphate-buffered saline (PBS), and analyzed using a Guava easyCyte single sample flow cytometer (Millipore). At indicated time points, NAD⁺ levels were measured using a NAD/NADH-Glo assay kit (Promega) according to the manufacturer's manual. The percentage of the NAD⁺ level was calculated by dividing the measured luminescence of tested strains with that of the control strains at the same time points. RPPX_26255 and RPPX_26260 were modeled using the I-TASSER server (35) and visualized using PyMol (version 2.3.1). Phylogenetic trees of toxin-antitoxin module derived from the COG5654-COG5642 family were constructed using MEGA (version 10.0.5) as a maximum likelihood tree with 100 bootstraps and visualized using the iTOL Web server (<https://itol.embl.de>) (45).

Data availability. The sequence data for wild-type *P. putida* S12 and plasmid-cured genotypes *P. putida* S12 ΔpTTS12 have been submitted to the SRA database under accession number PRJNA602416.

SUPPLEMENTAL MATERIAL

Supplemental material is available online only.

SUPPLEMENTAL FILE 1, PDF file, 7 MB.

ACKNOWLEDGMENTS

H.K. was supported by the Indonesia Endowment Fund for Education (LPDP) as scholarship provider from the Ministry of Finance, Indonesia. R.H. was funded by the Dutch National Organization for Scientific Research NWO, through the ERAnet-Industrial Biotechnology program, project "Pseudomonas 2.0."

REFERENCES

- Aono R, Kobayashi H. 1997. Cell surface properties of organic solvent-tolerant mutants of *Escherichia coli* K-12. *Appl Environ Microbiol* 63: 3637–3642. <https://doi.org/10.1128/AEM.63.9.3637-3642.1997>.
- Kabelitz N, Santos PM, Heipieper HJ. 2003. Effect of aliphatic alcohols on growth and degree of saturation of membrane lipids in *Acinetobacter calcoaceticus*. *FEMS Microbiol Lett* 220:223–227. [https://doi.org/10.1016/S0378-1097\(03\)00103-4](https://doi.org/10.1016/S0378-1097(03)00103-4).
- Hartmans S, van der Werf MJ, de Bont JA. 1990. Bacterial degradation of styrene involving a novel flavin adenine dinucleotide-dependent styrene monooxygenase. *Appl Environ Microbiol* 56:1347–1351. <https://doi.org/10.1128/AEM.56.5.1347-1351.1990>.
- Heipieper HJ, Weber FJ, Sikkema J, Keweloh H, de Bont J. 1994. Mechanisms of resistance of whole cells to toxic organic solvents. *Trends Biotechnol* 12:409–415. [https://doi.org/10.1016/0167-7799\(94\)90029-9](https://doi.org/10.1016/0167-7799(94)90029-9).
- Wierckx NJP, Ballerstedt H, de Bont JAM, Wery J. 2005. Engineering of solvent-tolerant *Pseudomonas putida* S12 for bioproduction of phenol from glucose. *Appl Environ Microbiol* 71:8221–8227. <https://doi.org/10.1128/AEM.71.12.8221-8227.2005>.
- Verhoef S, Wierckx N, Westerhof RGM, de Winde JH, Ruijsenaars HJ. 2009. Bioproduction of p-hydroxystyrene from glucose by the solvent-tolerant bacterium *Pseudomonas putida* S12 in a two-phase water-decanol fermentation. *Appl Environ Microbiol* 75:931–936. <https://doi.org/10.1128/AEM.02186-08>.
- Verhoef S, Ruijsenaars HJ, de Bont JAM, Wery J. 2007. Bioproduction of p-hydroxybenzoate from renewable feedstock by solvent-tolerant *Pseudomonas putida* S12. *J Biotechnol* 132:49–56. <https://doi.org/10.1016/j.jbiotec.2007.08.031>.
- Ruijsenaars HJ, Sperling E, Wiegerinck PHG, Brands FTL, Wery J, de Bont J. 2007. Testosterone 15beta-hydroxylation by solvent tolerant *Pseudomonas putida* S12. *J Biotechnol* 131:205–208. <https://doi.org/10.1016/j.jbiotec.2007.06.007>.
- Koopman F, Wierckx N, de Winde JH, Ruijsenaars HJ. 2010. Efficient whole-cell biotransformation of 5-(hydroxymethyl)furfural into FDCA, 2,5-furandicarboxylic acid. *Bioresour Technol* 101:6291–6296. <https://doi.org/10.1016/j.biortech.2010.03.050>.
- Volkers RJM, de Jong AL, Hulst AG, van Baar BLM, de Bont JAM, Wery J. 2006. Chemostat-based proteomic analysis of toluene-affected *Pseudomonas putida* S12. *Environ Microbiol* 8:1674–1679. <https://doi.org/10.1111/j.1462-2920.2006.01056.x>.
- Volkers RJM, Snoek LB, Ruijsenaars HJ, de Winde JH. 2015. Dynamic response of *Pseudomonas putida* S12 to sudden addition of toluene and the potential role of the solvent tolerance gene *trgl*. *PLoS One* 10: e0132416. <https://doi.org/10.1371/journal.pone.0132416>.
- Kuepper J, Ruijsenaars HJ, Blank LM, de Winde JH, Wierckx N. 2015. Complete genome sequence of solvent-tolerant *Pseudomonas putida* S12 including megaplasmid pTTS12. *J Biotechnol* 200:17–18. <https://doi.org/10.1016/j.jbiotec.2015.02.027>.
- Kieboom J, Dennis JJ, de Bont JAM, Zylstra GJ. 1998. Identification and molecular characterization of an efflux pump involved in *Pseudomonas*

- putida* S12 solvent tolerance. *J Biol Chem* 273:85–91. <https://doi.org/10.1074/jbc.273.1.85>.
14. Kieboom J, Dennis JJ, Zylstra GJ, de Bont JA. 1998. Active efflux of organic solvents by *Pseudomonas putida* S12 is induced by solvents. *J Bacteriol* 180:6769–6772. <https://doi.org/10.1128/JB.180.24.6769-6772.1998>.
 15. Garikipati S, McIver AM, Peeples TL. 2009. Whole-cell biocatalysis for 1-naphthol production in liquid-liquid biphasic systems. *Appl Environ Microbiol* 75:6545–6552. <https://doi.org/10.1128/AEM.00434-09>.
 16. Janardhan Garikipati SVB, Peeples TL. 2015. Solvent resistance pumps of *Pseudomonas putida* S12: applications in 1-naphthol production and biocatalyst engineering. *J Biotechnol* 210:91–99. <https://doi.org/10.1016/j.jbiotec.2015.06.419>.
 17. O'Connor KE, Dobson AD, Hartmans S. 1997. Indigo formation by microorganisms expressing styrene monooxygenase activity. *Appl Environ Microbiol* 63:4287–4291. <https://doi.org/10.1128/AEM.63.11.4287-4291.1997>.
 18. Isken S, de Bont J. 2000. The solvent efflux system of *Pseudomonas putida*. *Appl Microbiol Biotechnol* 54:711–714. <https://doi.org/10.1007/s002530000453>.
 19. Shao Y, Harrison EM, Bi D, Tai C, He X, Ou HY, Rajakumar K, Deng Z. 2011. TADB: a web-based resource for type 2 toxin-antitoxin loci in bacteria and archaea. *Nucleic Acids Res* 39:D606–D611. <https://doi.org/10.1093/nar/gkq908>.
 20. Xie Y, Wei Y, Shen Y, Li X, Zhou H, Tai C, Deng Z, Ou HY. 2018. TADB 2.0: an updated database of bacterial type II toxin-antitoxin loci. *Nucleic Acids Res* 46:D749–D753. <https://doi.org/10.1093/nar/gkx1033>.
 21. Harms A, Brodersen DE, Mitarai N, Gerdes K. 2018. Toxins, targets, and triggers: an overview of toxin-antitoxin biology. *Mol Cell* 70:768–784. <https://doi.org/10.1016/j.molcel.2018.01.003>.
 22. Maisonneuve E, Gerdes K. 2014. Molecular mechanisms underlying bacterial persisters. *Cell* 157:539–548. <https://doi.org/10.1016/j.cell.2014.02.050>.
 23. McKenzie JL, Robson J, Berney M, Smith TC, Ruthe A, Gardner PP, Arcus VL, Cook GM. 2012. A VapBC toxin-antitoxin module is a posttranscriptional regulator of metabolic flux in *Mycobacteria*. *J Bacteriol* 194:2189–2204. <https://doi.org/10.1128/JB.06790-11>.
 24. Pinto UM, Pappas KM, Winans SC. 2012. The ABCs of plasmid replication and segregation. *Nat Rev Microbiol* 10:755–765. <https://doi.org/10.1038/nrmicro2882>.
 25. Trevors JT. 1986. Plasmid curing in bacteria. *FEMS Microbiol Lett* 32:149–157. <https://doi.org/10.1111/j.1574-6968.1986.tb01189.x>.
 26. Chakrabarty AM. 1972. Genetic basis of the biodegradation of salicylate in *Pseudomonas*. *J Bacteriol* 112:815–823. <https://doi.org/10.1128/JB.112.2.815-823.1972>.
 27. Wynands B, Lenzen C, Otto M, Koch F, Blank LM, Wierckx N. 2018. Metabolic engineering of *Pseudomonas taiwanensis* VLB120 with minimal genomic modifications for high-yield phenol production. *Metab Eng* 47:121–133. <https://doi.org/10.1016/j.ymben.2018.03.011>.
 28. Nikel PI, de Lorenzo V. 2018. *Pseudomonas putida* as a functional chassis for industrial biocatalysis: from native biochemistry to trans-metabolism. *Metab Eng* 50:142–155. <https://doi.org/10.1016/j.ymben.2018.05.005>.
 29. Studier FW, Moffatt BA. 1986. Use of bacteriophage T7 RNA polymerase to direct selective high-level expression of cloned genes. *J Mol Biol* 189:113–130. [https://doi.org/10.1016/0022-2836\(86\)90385-2](https://doi.org/10.1016/0022-2836(86)90385-2).
 30. Puigbò P, Bravo IG, Garcia-Vallve S. 2008. CAIcal: a combined set of tools to assess codon usage adaptation. *Biol Direct* 3:38. <https://doi.org/10.1186/1745-6150-3-38>.
 31. Makarova KS, Wolf YI, Koonin EV. 2009. Comprehensive comparative-genomic analysis of Type 2 toxin-antitoxin systems and related mobile stress response systems in prokaryotes. *Biol Direct* 4:19. <https://doi.org/10.1186/1745-6150-4-19>.
 32. Piscotta FJ, Jeffrey PD, Link AJ. 2019. ParST is a widespread toxin-antitoxin module that targets nucleotide metabolism. *Proc Natl Acad Sci U S A* 116:826–834. <https://doi.org/10.1073/pnas.1814633116>.
 33. Skjerming RB, Senissar M, Winther KS, Gerdes K, Brodersen DE. 2019. The RES domain toxins of RES-Xre toxin-antitoxin modules induce cell stasis by degrading NAD⁺. *Mol Microbiol* 111:221–236. <https://doi.org/10.1111/mmi.14150>.
 34. Freire DM, Gutierrez C, Garza-Garcia A, Grabowska AD, Sala AJ, Ariyachanokun K, Panikova T, Beckham KSH, Colom A, Pogenberg V, Cianci M, Tuukkanen A, Boudehen YM, Peixoto A, Botella L, Svergun DI, Schnappinger D, Schneider TR, Genevoux P, de Carvalho LPS, Wilmanns M, Parret AHA, Neyrolles O. 2019. An NAD⁺ phosphorylase toxin triggers *Mycobacterium tuberculosis* cell death. *Mol Cell* 73:1282–1291.e8. <https://doi.org/10.1016/j.molcel.2019.01.028>.
 35. Yang J, Yan R, Roy A, Xu D, Poisson J, Zhang Y. 2015. The I-TASSER suite: protein structure and function prediction. *Nat Methods* 12:7–8. <https://doi.org/10.1038/nmeth.3213>.
 36. Murphy JR. 2011. Mechanism of diphtheria toxin catalytic domain delivery to the eukaryotic cell cytosol and the cellular factors that directly participate in the process. *Toxins (Basel)* 3:294–308. <https://doi.org/10.3390/toxins3030294>.
 37. Martínez-García E, de Lorenzo V. 2011. Engineering multiple genomic deletions in Gram-negative bacteria: analysis of the multi-resistant antibiotic profile of *Pseudomonas putida* KT2440. *Environ Microbiol* 13:2702–2716. <https://doi.org/10.1111/j.1462-2920.2011.02538.x>.
 38. Holtwick R, Meinhardt F, Keweloh H. 1997. *cis-trans* isomerization of unsaturated fatty acids: cloning and sequencing of the *cti* gene from *Pseudomonas putida* P8. *Appl Environ Microbiol* 63:4292–4297. <https://doi.org/10.1128/AEM.63.11.4292-4297.1997>.
 39. Blank LM, Ionidis G, Ebert BE, Bühler B, Schmid A. 2008. Metabolic response of *Pseudomonas putida* during redox biocatalysis in the presence of a second octanol phase. *FEBS J* 275:5173–5190. <https://doi.org/10.1111/j.1742-4658.2008.06648.x>.
 40. Ebert BE, Kurth F, Grund M, Blank LM, Schmid A. 2011. Response of *Pseudomonas putida* KT2440 to increased NADH and ATP demand. *Appl Environ Microbiol* 77:6597–6605. <https://doi.org/10.1128/AEM.05588-11>.
 41. Pullinger GD, Lax AJ. 1992. A *Salmonella dublin* virulence plasmid locus that affects bacterial growth under nutrient-limited conditions. *Mol Microbiol* 6:1631–1643. <https://doi.org/10.1111/j.1365-2958.1992.tb00888.x>.
 42. Zhang YX, Li J, Guo XK, Wu C, Bi B, Ren SX, Wu CF, Zhao GP. 2004. Characterization of a novel toxin-antitoxin module, VapBC, encoded by *Leptospira interrogans* chromosome. *Cell Res* 14:208–216. <https://doi.org/10.1038/sj.cr.7290221>.
 43. Abril MA, Michan C, Timmis KN, Ramos JL. 1989. Regulator and enzyme specificities of the TOL plasmid-encoded upper pathway for degradation of aromatic hydrocarbons and expansion of the substrate range of the pathway. *J Bacteriol* 171:6782–6790. <https://doi.org/10.1128/jb.171.12.6782-6790.1989>.
 44. Zobel S, Benedetti I, Eisenbach L, de Lorenzo V, Wierckx N, Blank LM. 2015. Tn7-based device for calibrated heterologous gene expression in *Pseudomonas putida*. *ACS Synth Biol* 4:1341–1351. <https://doi.org/10.1021/acssynbio.5b00058>.
 45. Letunic I, Bork P. 2019. Interactive Tree Of Life (iTOL) v4: recent updates and new developments. *Nucleic Acids Res* 47:W256–W259. <https://doi.org/10.1093/nar/gkz239>.
 46. Bagdasarian M, Lurz R, Rückert B, Franklin FCH, Bagdasarian MM, Frey J, Timmis KN. 1981. Specific-purpose plasmid cloning vectors II. Broad host range, high copy number, RSF 1010-derived vectors, and a host-vector system for gene cloning in *Pseudomonas*. *Gene* 16:237–247. [https://doi.org/10.1016/0378-1119\(81\)90080-9](https://doi.org/10.1016/0378-1119(81)90080-9).
 47. Boyer HW, Roulland-Dussoix D. 1969. A complementation analysis of the restriction and modification of DNA in *Escherichia coli*. *J Mol Biol* 41:459–472. [https://doi.org/10.1016/0022-2836\(69\)90288-5](https://doi.org/10.1016/0022-2836(69)90288-5).
 48. Herrero M, De Lorenzo V, Timmis KN. 1990. Transposon vectors containing non-antibiotic resistance selection markers for cloning and stable chromosomal insertion of foreign genes in gram-negative bacteria. *J Bacteriol* 172:6557–6567. <https://doi.org/10.1128/jb.172.11.6557-6567.1990>.
 49. Figurski DH, Helinski DR. 1979. Replication of an origin-containing derivative of plasmid RK2 dependent on a plasmid function provided in *trans*. *Proc Natl Acad Sci U S A* 76:1648–1652. <https://doi.org/10.1073/pnas.76.4.1648>.
 50. Choi K-H, Gaynor JB, White KG, Lopez C, Bosio CM, Karkhoff-Schweizer RR, Schweizer HP. 2005. A Tn7-based broad-range bacterial cloning and expression system. *Nat Methods* 2:443–448. <https://doi.org/10.1038/nmeth765>.